MECHANICS
МЕХАНИКА

UDC 620.17.4
https://doi.org/10.23947/2687-1653-2024-24-3-215-226

Original Empirical Research

Increasing the Interlayer Fracture Toughness of Polymer Fabric Composites Using Local 3D-Reinforcement (Felting)

Galina A. Forental[1] ✉, **Sergey B. Sapozhnikov**[1,2]
[1] South Ural State University, Chelyabinsk, Russian Federation
[2] Central Aerohydrodynamic Institute, Zhukovsky, Russian Federation
✉gforental@mail.ru

EDN: KVEMQM

Abstract

Introduction. One of the reasons for undesirable delamination of polymer composites with fabric reinforcement is low transverse shear properties. It is known that the reinforcement of polymer fabric composites in the *Z* direction reduces the sensitivity to delamination and increases the viscosity of interlayer fracture. Various methods of three-dimensional reinforcement of polymer fabric composites are proposed in the literature. However, they complicate the manufacturing process of the structure. The problem is solved by the method of three-dimensional reinforcement proposed in this article — felting. This is a local reinforcement of the composite in the *Z* direction with minimal production changes. The degree of *Z*-reinforcement is determined by the felting density, i.e., the number of needle punches per 1 cm^2 of the fabric package. The work is aimed at evaluating the effect of felting on the interlayer crack resistance of a composite material.

Materials and Methods. The interlayer fracture toughness G_{IIc} was determined on a cross-woven fiberglass with felting of 10 cm^{-2}. The material was impregnated with Etal-370 resin and Etal-45 hardener. Experiments according to ASTM D7905M–14 and GOST 33685–2015 standards were carried out on an Instron 5900R test machine. The stress state at the crack tip was analyzed with regard to the nonlocal strength theory in the ANSYS Workbench program (option "static strength analysis"). The finite element method (FEM) was used.

Results. The "load — displacement" curves were considered for the samples. Values G_{IIc} were calculated. The results of ENF tests for felting density of 0 cm^{-2} and 10 cm^{-2} were summarized. Control samples and felting samples were compared. In the latter case, G_{IIc} turned out to be ~33% higher. The stress state at the crack tip was calculated under DCB and ENF loading. The dependences of maximum normal and shear stresses, as well as displacements, were visualized in the form of graphs and color charts. To get the calculated "load — displacement" dependences using FEM, the reverse method of obtaining transverse shear constants was used. DCB loading showed that felting provided increasing the rupture strength in the *Z* direction to ~18%, by 39 to 46 MPa, and in the planes *XZ*— to ~16%, by 77 to 89 MPa.

Discussion and Conclusion. Felting as a method of local three-dimensional reinforcement enhances the interlayer crack resistance of polymer fabric composites. It provides reducing the area of stratifications after local impacts during the operation of structures. Flexible felting technology makes it possible to create zones with an arbitrary impact density, increasing fracture toughness only in the required places of structures. The FEM analysis of the stress state at the crack tip within the framework of the nonlocal strength theory has shown that in strength calculations, the stratification crack can be considered as a stress concentrator.

Keywords: reinforcement of polymer fabric composites, transverse shear strength, interlayer crack resistance, interlaminar fracture toughness, felting local three-dimensional reinforcement

Acknowledgements. The authors would like to thank colleagues A.V. Nikonov and A.V. Kheruvimov for their help in preparing the samples.

Funding Information. The research was done within the framework of the Program for the Creation and Development of the World-Class Scientific Center "Supersound" for 2020–2025 with the financial support of the Ministry of Education and Science of the Russian Federation (Agreement no. 075–15–2022–1023, dated May 17, 2022).

For Citation. Forental GA, Sapozhnikov SB. Increasing the Interlayer Fracture Toughness of Polymer Fabric Composites Using Local 3D-Reinforcement (Felting). *Advanced Engineering Research* (*Rostov-on-Don*). 2024;24(3):215–226. https://doi.org/10.23947/2687-1653-2024-24-3-215-226

Оригинальное эмпирическое исследование

Повышение межслойной трещиностойкости полимерных тканевых композитов с помощью локального трехмерного армирования (фелтинга)

Г.А. Форенталь[1] ✉, **С.Б. Сапожников**[1,2]

[1] Южно-Уральский государственный университет, г. Челябинск, Российская Федерация

[2] Центральный аэрогидродинамический институт имени профессора Н.Е. Жуковского, г. Жуковский, Российская Федерация

✉gforental@mail.ru

Аннотация

Введение. Одна из причин нежелательных расслоений полимерных композитов с тканевым армированием — низкие трансверсально-сдвиговые характеристики. Известно, что армирование полимерных тканевых композитов в направлении *Z* уменьшает чувствительность к расслоению и повышает вязкость межслойного разрушения. В литературе предлагаются разные способы трехмерного армирования полимерных тканевых композитов. Однако они усложняют процесс изготовления конструкции. Проблему решает предложенный в данной статье способ трехмерного армирования — фелтинг. Это локальное армирование композита в направлении *Z* при минимальных производственных изменениях. Степень *Z*-армирования определяется плотностью фелтинга, т.е. количеством ударов иглы на 1 см^2 тканевого пакета. Цель работы — оценить влияние фелтинга на межслойную трещиностойкость композитного материала.

Материалы и методы. Межслойную вязкость разрушения G_{IIc} определяли на стеклоткани полотняного переплетения с фелтингом 10 см$^{-2}$. Материал пропитывали смолой Этал-370 и отвердителем Этал-45. Эксперименты по стандартам ASTM D7905M–14 и ГОСТ 33685–2015 проводили на испытательной машине Instron 5900R. Напряженное состояние у вершины трещины анализировали с позиции нелокальной теории прочности в программе Ansys Workbench (опция «статический прочностной анализ»). Задействовали метод конечных элементов (МКЭ).

Результаты исследования. Для образцов рассмотрели кривые «нагрузка — перемещение». Вычислили значения G_{IIc}. Обобщили итоги ENF-испытаний для плотности фелтинга 0 см$^{-2}$ и 10 см$^{-2}$. Сравнили контрольные образцы и образцы с фелтингом. В последнем случае G_{IIc} оказалась выше на ~33 %. Рассчитали напряженное состояние у вершины трещины при DCB- и ENF-нагружении. Визуализировали в виде графиков и цветовых диаграмм зависимости максимальных нормальных и касательных напряжений, а также перемещений. Для получения расчетных зависимостей «нагрузка — перемещение» с помощью МКЭ использовали обратный метод получения трансверсально-сдвиговых констант. Нагружение по схеме DCB показало, что фелтинг позволяет увеличить предел прочности на растяжение в направлении *Z* на ~18 %, с 39 до 46 МПа, а в плоскости *XZ* — на ~16 %, с 77 МПа до 89 МПа.

Обсуждение и заключение. Фелтинг как способ локального трехмерного армирования усиливает межслойную трещиностойкость полимерных тканевых композитов. Он позволяет сократить площадь расслоений после локальных ударов при эксплуатации конструкций. Гибкая технология фелтинга дает возможность создавать зоны с произвольной плотностью ударов, повышая трещиностойкость лишь в необходимых местах конструкций. МКЭ-анализ напряженного состояния у вершины трещины в рамках нелокальной теории прочности показал, что в прочностных расчетах трещину расслоения можно рассматривать как концентратор напряжений.

Ключевые слова: армирование полимерных тканевых композитов, трансверсально-сдвиговая прочность, межслойная трещиностойкость, межслоевая вязкость разрушения, фелтинговое локальное трехмерное армирование

Благодарности. Авторы выражают признательность коллегам Никонову А.В., Херувимову А.В. за помощь в изготовлении образцов для экспериментальных исследований.

Финансирование. Исследование выполнено в рамках Программы создания и развития научного центра мирового уровня «Сверхзвук» на 2020–2025 годы при финансовой поддержке Минобрнауки России (соглашение от 17 мая 2022 г. № 075–15–2022–1023).

Для цитирования. Форенталь Г.А., Сапожников С.Б. Повышение межслойной трещиностойкости полимерных тканевых композитов с помощью локального трехмерного армирования (фелтинга). *Advanced Engineering Research* (*Rostov-on-Don*). 2024;24(3):215–226. https://doi.org/10.23947/2687-1653-2024-24-3-215-226

Introduction. Fibrous polymer composites are widely used, in particular, in aviation and space engineering due to their significant rigidity and strength in the fiber orientation (plane *XY*) [1]. However, the transverse shear strength of these materials is quite low [2], as it is determined by the features of the polymer matrix [3]. Reinforcement of polymer fabric composites in the *Z* direction provides reducing the sensitivity to delamination, i.e., increasing the viscosity of interlayer fracture [4].

Various methods of three-dimensional reinforcement of polymer fabric composites are known [5]. However, they create additional difficulties in the manufacture of structures made of polymer fabric composites [6]. The method of three-dimensional reinforcement proposed in this work, felting [7], makes it possible to obtain a locally reinforced composite in the *Z* direction with minimal changes in the production process. The degree of Z-reinforcement is determined by the felting density, i.e., the number of needle punches per 1 cm^2 of the area of the fabric package [8].

The use of various methods for determining the fracture toughness of polymer composite materials [9] makes it possible to conduct studies on various samples [10] and with different loading methods [11]. One of the most common approaches is the three-point bending method. In this case, a beam-shaped delamination sample is used. We are talking about ENF tests (End-Notched Flexure — bending of a sample with edge delamination) [12], which involve transverse shear loading. This makes it possible to determine the interlayer fracture viscosity of G_{IIc} — mode II fracture. High shear stresses occur at the crack tip [13].

Another common way to determine transverse characteristics is the Double Cantilever Beam method (DCB tests). In DCB tests, the value of the interlaminar fracture toughness G_{Ic} is determined under separation loading — fracture according to mode I [14]. The delamination crack spreads due to the action of normal stresses [15].

The presented work was aimed at the evaluation of the effect of felting on the interlayer fracture toughness of a composite material. To do this, ENF tests (bending of a sample with an edge separation) of a composite material with increased crack resistance due to the use of felting were carried out. Previously, the authors studied the effect of felting on the interlayer crack resistance of a composite material during DCB tests [16]. A computational model based on the nonlocal theory of strength has been developed. It provides for the calculation of the stresses that occur in ENF and DCB samples, for cracks of various lengths, using the finite element method (FEM).

Materials and Methods

Experimental determination of interlayer crack resistance by the ENF method. The samples were made of cross-woven fiberglass with a layer thickness of 0.2 mm. A package of dry two-layered fiberglass was punched on a felting machine with a felting density of 10 cm^{-2} (10 punches with a felting machine needle per 1 cm^2 of dry glass fabric). The fiberglass package was punched in such a way that after impregnation and hardening, the initial crack did not fall on the felting area. To create an initial crack between two layers of fiberglass, an aluminum foil with a thickness of 11 μm, coated with a Vs-M parting lubricant, was placed. Fiberglass was impregnated with resin Etal-370 and hardener Etal-45. For the production of reference samples, two layers of dry fiberglass were impregnated with Etal-370 resin and Etal-45 hardener without punching on a felting machine. After impregnation, plates from glass textolite STEF (electrotechnical glass-cloth-base laminate) were glued to two layers of fiberglass (Fig. 1 *a*). Samples with a length of 150 mm and a width of 16 mm were obtained by cutting the hardened plates using a high-speed circular saw.

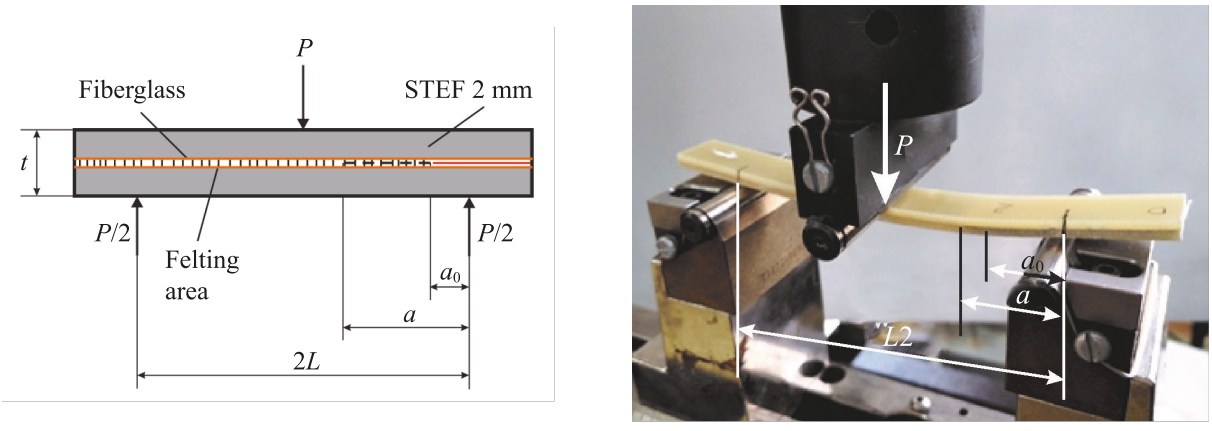

a) *b*)

Fig. 1. Configuration and parameters of ENF tests according to mode *II*:
a — loading scheme; *b* — photo of tests

The Instron 5900R test machine with a loading speed of 10 mm/min was used. The distance between the supports was $2L = 100$ mm. The initial crack length for all samples was $a_0 = 25$ mm. To perform compliance calibration over a wide range of crack lengths, one sample of each type was unloaded and reloaded. The resulting crack served as the initial crack in the next loading cycle.

Calibration recommended by ASTM D7905M–14[1] and GOST 33685–2015[2] standards was used to process the test results. This approach provided determining parameters A and m for each felting sample and each non-felting control sample from the linear dependence of two quantities — compliance of sample C and cube of the crack length a^3:

$$C\left(\delta/P(\delta)\right) = A + m \cdot a^3, \tag{1}$$

where P — load applied to the sample; δ — displacement.

After calibration and determination of parameters A and m, the crack length can be found from expression (1):

$$a = \left(\frac{C - A}{m}\right)^{1/3}. \tag{2}$$

The moment of the delamination onset is determined by the condition $C(\delta) = C(P_{max})$. Value of the interlayer fracture toughness at the separation onset (crack development):

$$G_{IIc} = \frac{3m \cdot P_{max}^2 \cdot a^2}{2b}, \tag{3}$$

where P_{max} — maximum load; a — crack length calculated by formula (2) at load P_{max}; b — sample width.

Calculation of the stress state at the crack tip under loading according to the DCB and ENF schemes. The stress state of a crack-like concentrator is estimated from the perspective of approaches that use nonlocal stresses [17], i.e., averaged on some basis [18]. The calculation model also includes the assumption of linear-elastic behavior of the material up to destruction [16].

The main hypothesis is that the strength criterion of the composite, which includes all components of stress averaged on the basis λ, is responsible for the development of a crack-like concentrator (Fig. 2):

$$\left(\frac{max\,\sigma_{z\lambda}}{Z_t}\right)^2 + \left(\frac{max\,\sigma_{x\lambda}}{X_t}\right)^2 + \left(\frac{max\,\tau_{xz\lambda}}{S}\right)^2 - \frac{max\,\sigma_{z\lambda} \cdot max\,\sigma_{x\lambda}}{Z_t \cdot X_t} \le 1, \tag{4}$$

where Z_t and X_t — rupture strength in the Z and X directions; S — shear strength in the plane XZ.

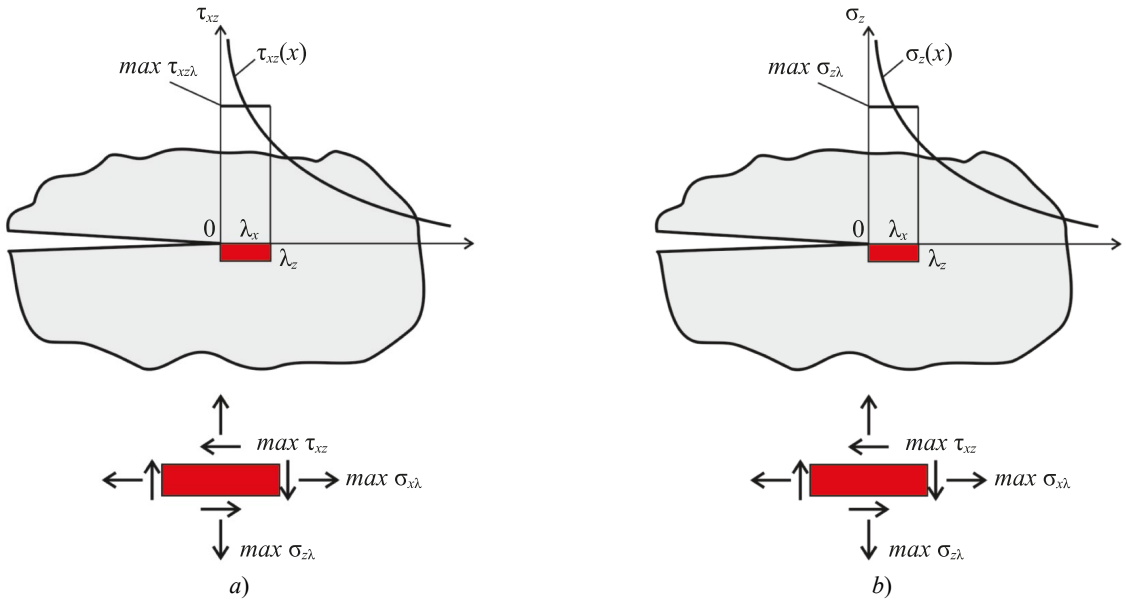

Fig. 2. Stresses averaged on the basis λ at the crack tip:
a — ENF tests; *b* — DCB tests

[1] ASTM D7905/D7905M–14. *Standard Test Method for Determination of the Mode II Interlaminar Fracture Toughness of Unidirectional Fiber-Reinforced Polymer Matrix Composites.* URL: https://cdn.standards.iteh.ai/samples/89096/03be6b5e53664f13a8703bb4342d981a/ASTM-D7905-D7905M-14.pdf (accessed: 22.04.2024).

[2] GOST 33685–2015. *Polymer Composites. Test Method for Determination of the Interlaminar Fracture Toughness under Shear.* (In Russ.) URL: https://docs.cntd.ru/document/1200127774 (accessed: 22.04.2024).

Due to the presence of symmetry planes, a three-dimensional 1/2 crack sample model was constructed for ENF loading (Fig. 3), and 1/4 crack sample — for DCB tests (Fig. 4). Calculations were performed in the ANSYS Workbench program (option “static structural”).

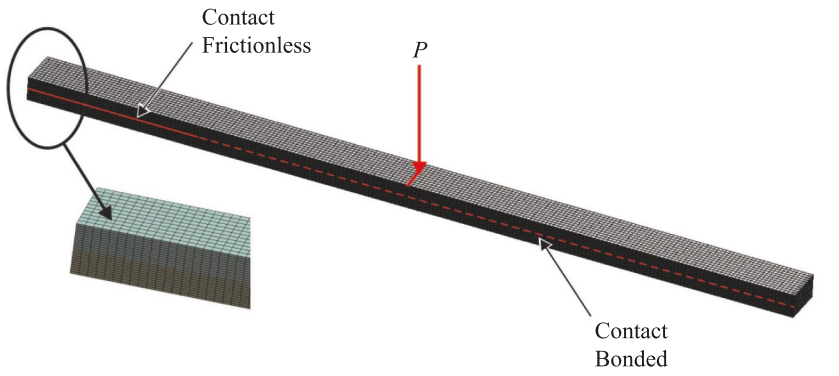

Fig. 3. Finite element model 1/2 of the sample and a fragment of the grid for ENF tests

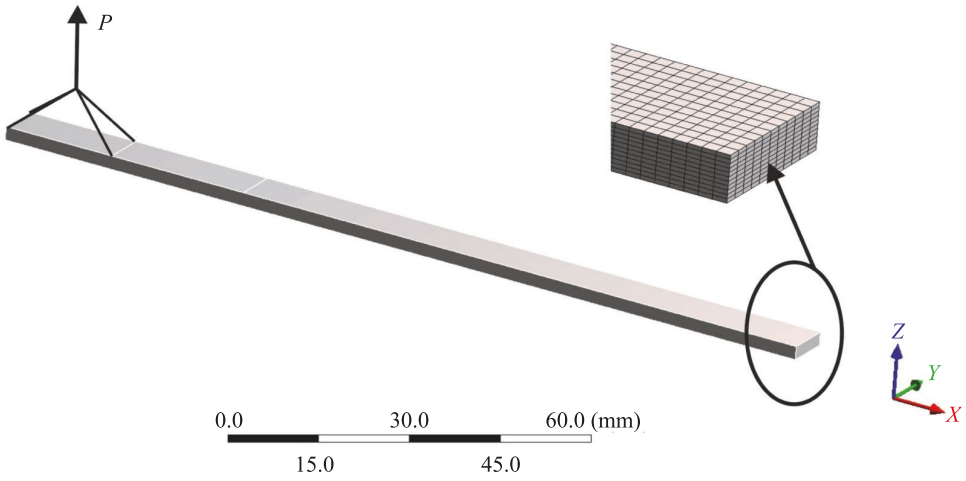

Fig. 4. Finite element model 1/4 of the sample and a fragment of the grid for DCB tests

When creating the finite element grid, parameter $\lambda_x = 0.75$ mm in width of the sample [19] and parameter $\lambda_z = 0.2$ mm in thickness of the sample were set, which corresponded to the thickness of the modified layer [20]. One finite element in the thickness of the layer was set in accordance with the layer wise theory used in assessing the strength of layers within the framework of mesomechanics of composites [21]. In ENF tests, the total displacements in the sample were much greater than the local displacements from the loading roller (Fig. 1 *b*); therefore, the grid of finite elements was not condensed at the places of application of loads and supports (Fig. 3). Properties of fiberglass used in the calculation:

- elastic modules $E_x = E_y = 23$ GPa, $E_z = 9$ GPa;
- shear modules $G_{xy} = G_{yz} = G_{xz} = 6000$ GPa;
- Poisson's coefficients $\mu_{xy} = 0.15$, $\mu_{yz} = \mu_{xz} = 0.3$ [22].

Since the volume fraction of transverse reinforcement is less than 1% [16], it is assumed in the calculations that the elastic properties of fiberglass do not change under felting.

Dependence $P(\delta)$ was calculated in accordance with the sequence described below.

1. FEM-calculation of the maximum stresses $max\sigma_{z\lambda}$, $max\sigma_{x\lambda}$ and $max\tau_{xz\lambda}$ and displacements of point δ of application of load $P = 1$ H for cracks with the given lengths in the range $a = 20…90$ mm (DCB) and $a = 25…40$ mm (ENF) was performed.

1. Approximation dependences $\sigma_{z\lambda} = f(a, P) = P{\cdot}b_1{\cdot}a$; $\sigma_{x\lambda} = f(a, P) = P{\cdot}b_2{\cdot}a$; $\tau_{xz\lambda} = f(a, P) = P{\cdot}b_3{\cdot}a$; $\delta = f(a, P) = P{\cdot}c_1{\cdot}a^3{\cdot}$(DCB) and $\sigma_{z\lambda} = f(a, P) = P{\cdot}b_1{\cdot}a$; $\sigma_{x\lambda} = f(a, P) = P{\cdot}b_2{\cdot}a$; $\tau_{xz\lambda} = f(a, P) = P{\cdot}(b_3{\cdot}a + d_3)$; $\delta = f(a, P) = P{\cdot}(c_1{\cdot}a^3 + c_2{\cdot}a^2 + c_3{\cdot}a + c_4){\cdot}$(ENF).

2. were constructed using the least squares method.

3. Load $P_{cr}(a_0)$ and displacement δ_{cr}, at which the initial crack length a_0 would increase abruptly by $\lambda_x = 0.75$ mm upon the violation of the strength criterion, were determined (4).

4. With crack length $a_0+n\lambda$, loads $P(a_0+n\lambda)$ and displacements $\delta(n)$ for $n>0$ were determined.

Research Results

Results of the experimental determination of interlayer fracture toughness by the ENF method. Figure 5 shows the "load — displacement" curves for all tested samples. All "load — displacement" curves have an area with constant compliance (C_{lin}), corresponding to the linear "load — displacement" ratio. Values C_{lin} were used for calibration.

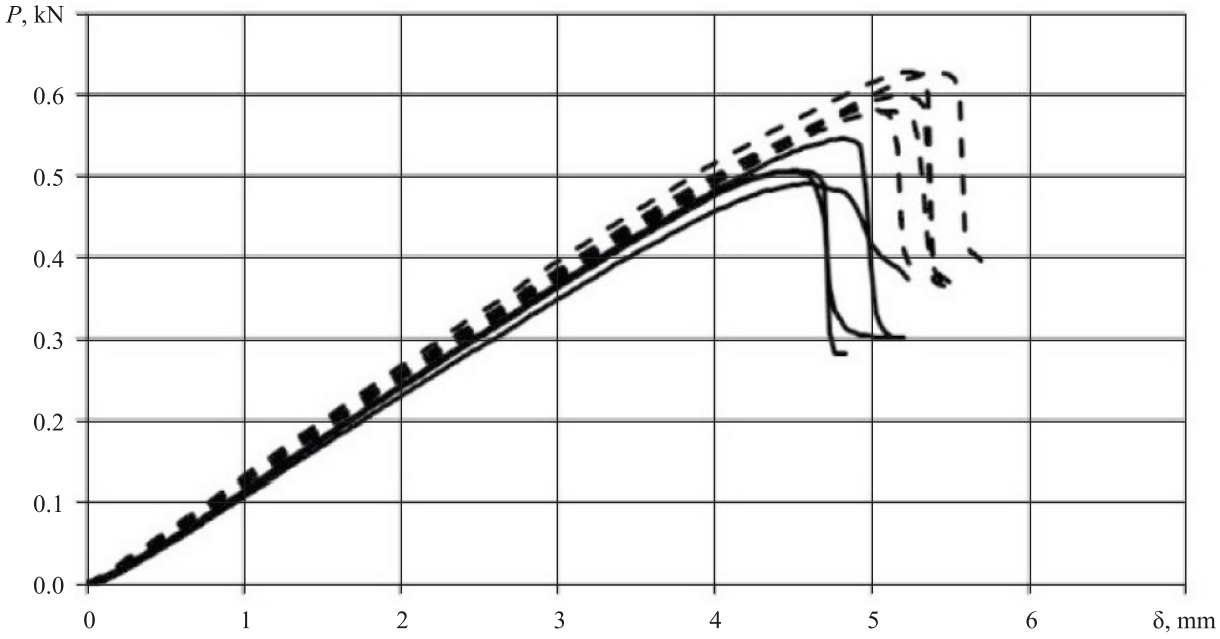

Fig. 5. "Load — displacement" diagrams of ENF tests
——— without felting; — — — — with felting

Figure 6 shows the calibration curves. For felting and non-felting samples, compliance is proportional to the cube of the crack length.

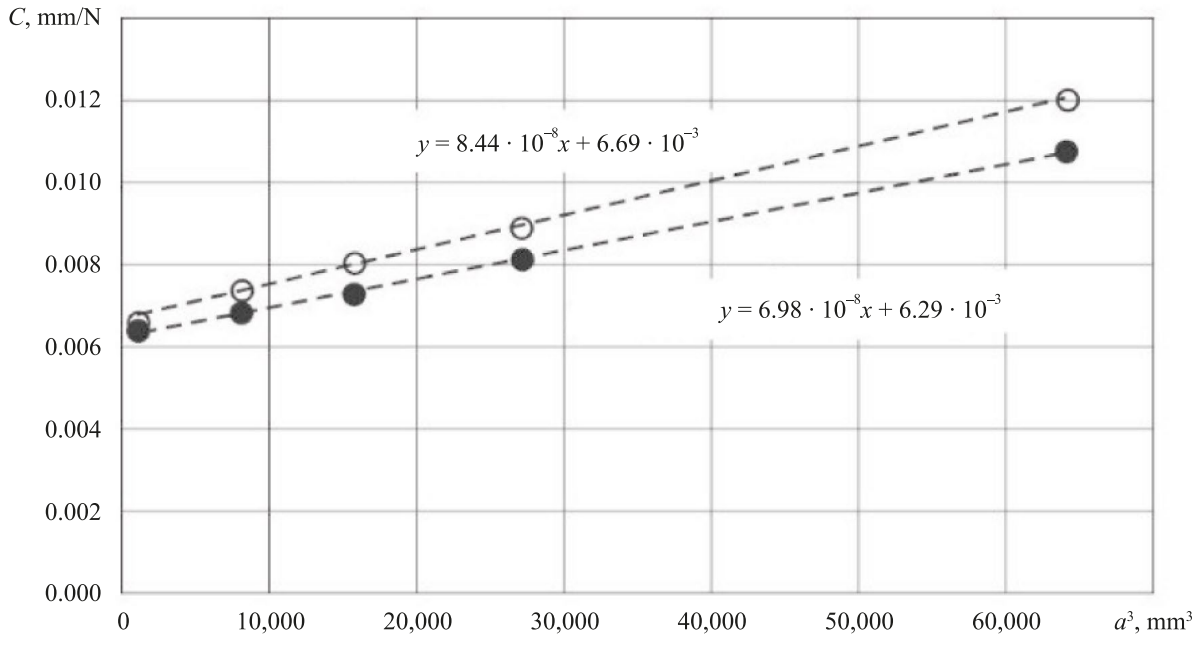

Fig. 6. Dependence of compliance of sample C on the cube of crack length a^3:
○ — without felting; ● — with felting

To calculate values of the crack length a^*, corresponding to the compliance at the delamination onset $C(P_{max})$, the obtained calibration curves and equation (2) were used. For the found values of the crack length a^*, values G_{IIc} were calculated using equation (3). The results are shown in Table 1.

Table 1

ENF Test Results

Felting Density, cm^{-2}	a_0, mm	C_{lin}, mm/N	$C_{(Pmax)}$, mm/N	a*, mm	P_{max}, N	G_{IIc}, kJ/m^2	G_{IIc} (average value), kJ/m^2 (CV)
0	25	8.032	8.845	29.4	504.6	1.723	1.840 ± 0.126 (6.9%)
0	25	7.980	8.807	29.3	544.6	1.983	
0	25	8.299	9.392	31.7	489.4	1.908	
0	25	7.905	8.900	29.7	505.2	1.746	
10	25	7.587	8.337	30.8	627.3	2.432	2.441 ± 0.154 (6.3%)
10	25	7.849	8.677	32.4	625.8	2.682	
10	25	7.937	8.811	33.0	578.4	2.376	
10	25	7.824	8.594	32.1	581.4	2.261	
10	25	7.880	8.818	33.1	589.3	2.456	
* variation coefficient							

Felting samples showed a significant (by ~33%) increase in the interlayer fracture toughness G_{IIc} compared to the control samples. After testing, felting samples were separated with a sharp knife and examined under a microscope. Micrographs of the zone without felting (area of the initial crack) and the zone with felting (area of crack development) are shown in Figure 7. When cracks develop, the fibers elongated during felting are destroyed, because their length is greater than the critical one [16].

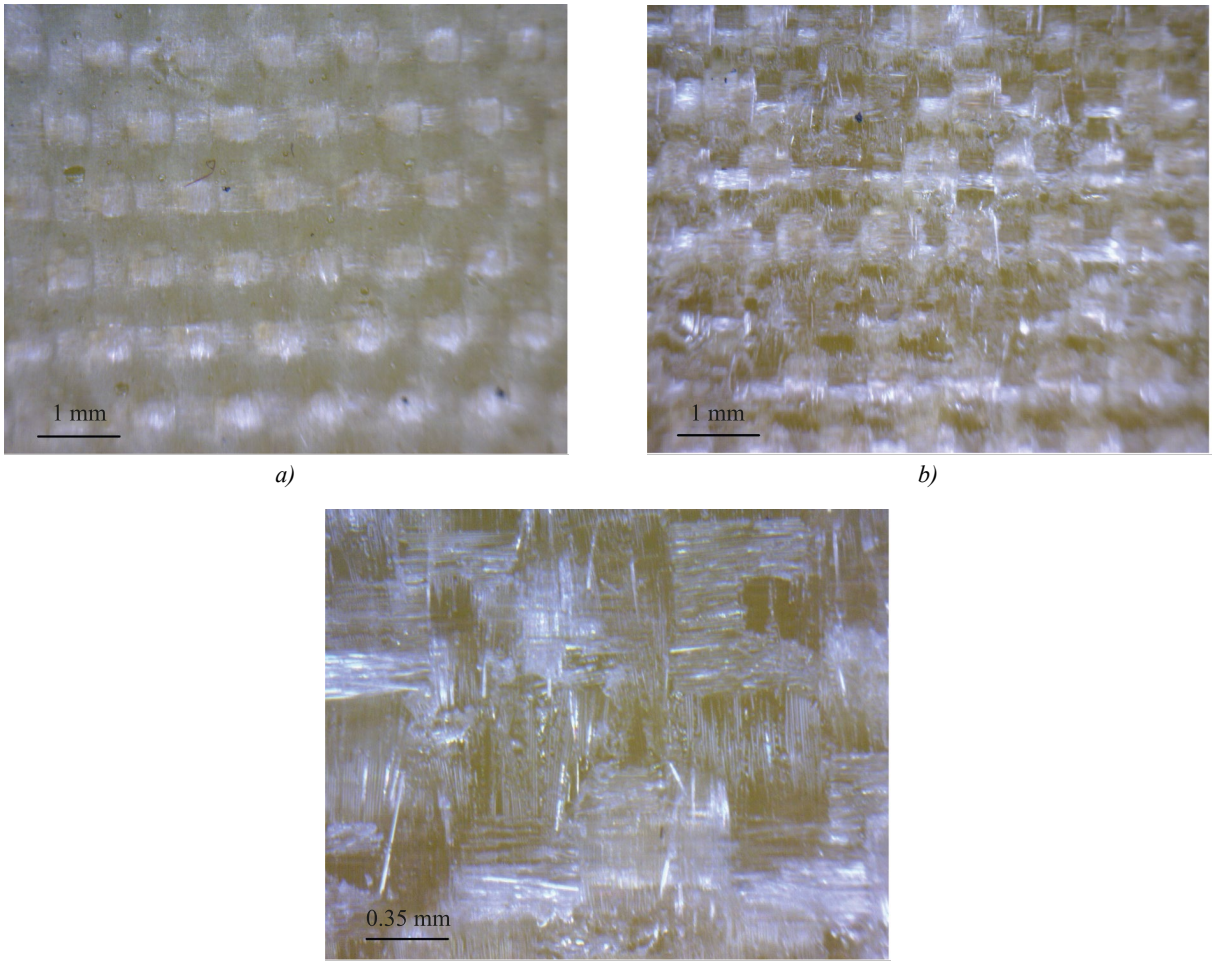

a) *b)* *c)*

Fig. 7. Micrographs of felting samples after ENF tests:
a — zone without felting (area of initial crack);
b — zone with felting (area of crack development);
c — zone with felting (enlarged scale)

Results of the calculation of the stress state at the crack tip under loading according to the DCB and ENF schemes. Figures 8–9 show the dependences of stress $max\sigma_{z\lambda}(a)$, $max\sigma_{x\lambda}(a)$, $max\tau_{xz\lambda}(a)$ and displacements $\delta(a)$. Conditions: $P = 1$ N, loading according to DCB and ENF schemes.

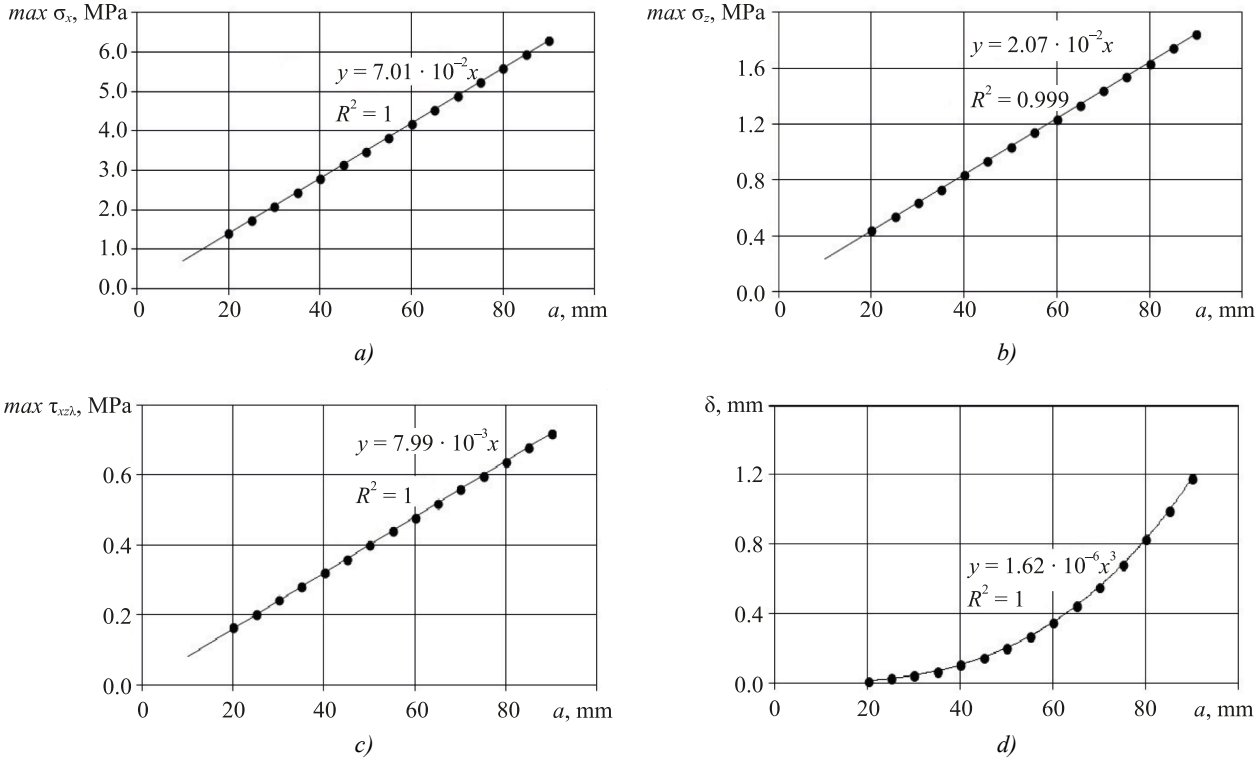

Fig. 8. DCB-loading. Dependences of maximum stresses and displacements of the crack length at $P = 1$ N:
a— dependence of normal stresses $max\sigma_{x\lambda}(a)$; *b* — dependence of normal stresses $max\sigma_{z\lambda}(a)$;
c — dependence of shear stresses $max\tau_{xz\lambda}(a)$; *d* — dependence of displacements $\delta(a)$

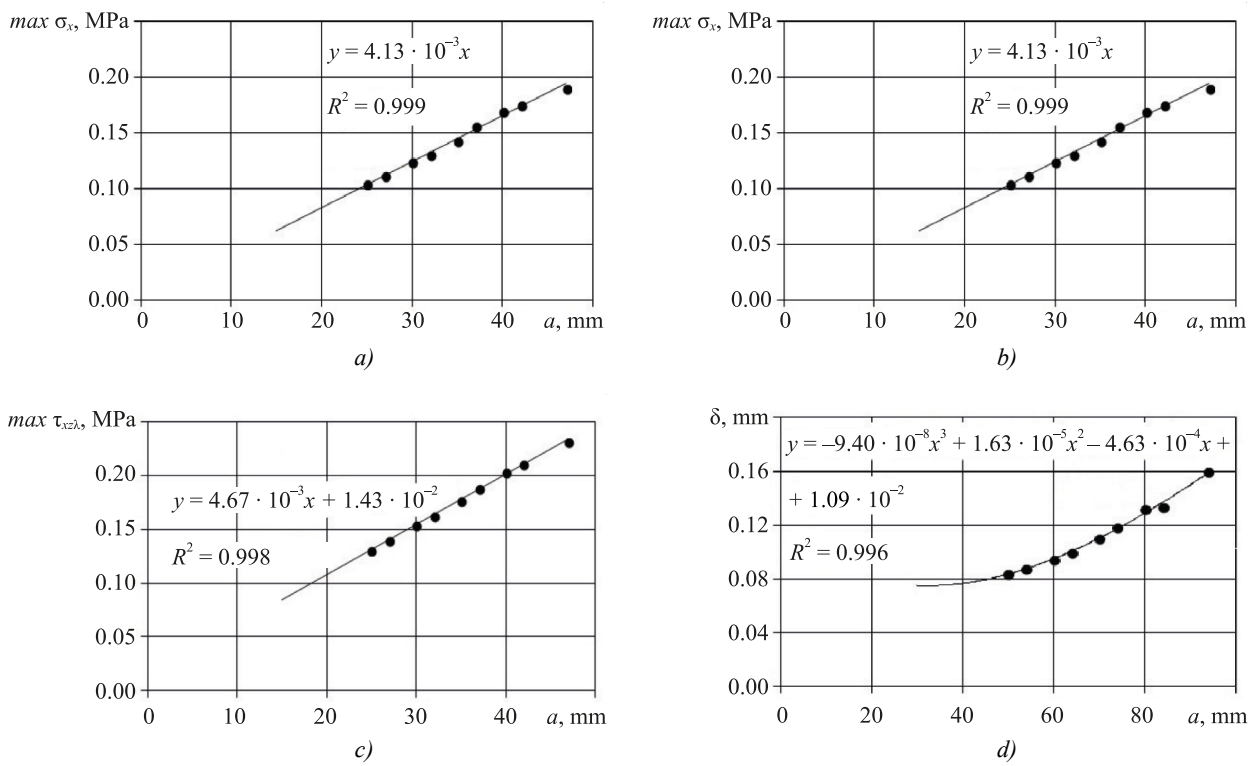

Fig. 9. ENF- loading. Dependences of maximum stresses and displacements of the crack length at $P = 1$ N:
a — dependence of normal stresses $max\sigma_{x\lambda}(a)$; *b* — dependence of normal stresses $max\sigma_{z\lambda}(a)$;
c — dependence of shear stresses $max\tau_{xz\lambda}(a)$; *d* — dependence of displacements $\delta(a)$

Examples of stress distribution at the crack tip are shown in Figures 10–11 with crack length a_0 = 30 mm.

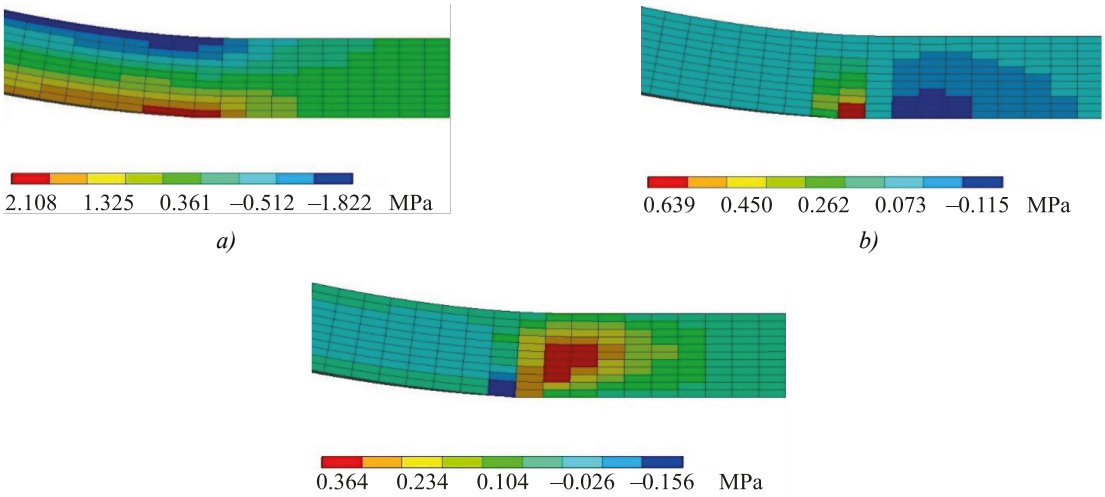

Fig. 10. Stresses at the crack tip under DCB loading: *a* — normal stresses $\sigma_{x\lambda}$; *b* — normal stresses $\sigma_{z\lambda}$; *c* — shear stresses $\tau_{xz\lambda}$

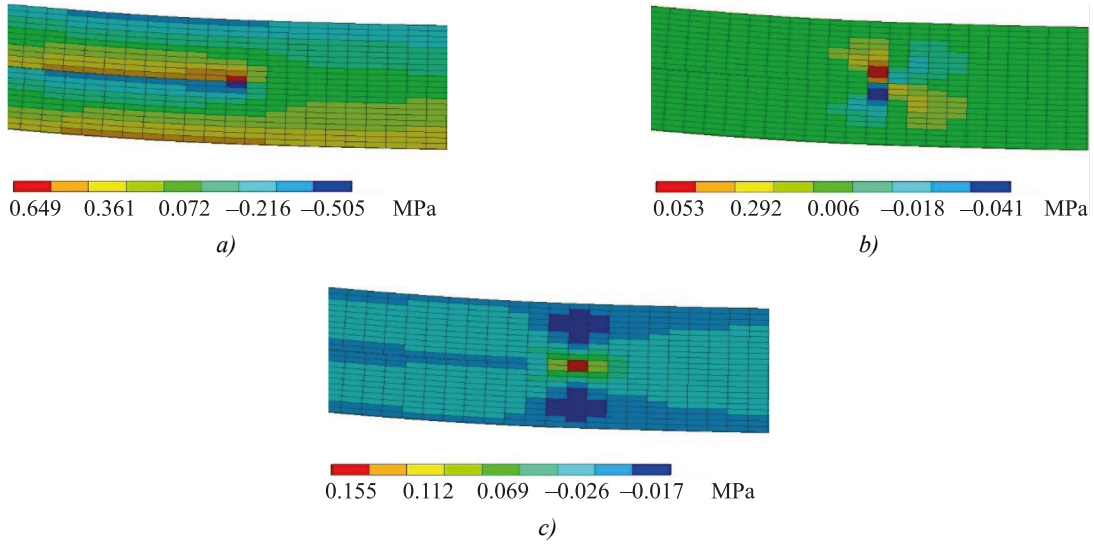

Fig. 11. Stresses at the crack tip under ENF loading: *a* — normal stresses $\sigma_{x\lambda}$; *b* — normal stresses $\sigma_{z\lambda}$; *c* — shear stresses $\tau_{xz\lambda}$

To obtain the calculated "load — displacement" dependences using FEM, the strength characteristics of the composite in the main directions are taken into account, i.e., criterion (4). Direct obtaining of transverse shear constants involves a certain difficulty; therefore, the reverse method is considered below. With this approach, the constants vary, and their best combination is found. This means that the calculated and experimental loading diagrams are in good agreement (mean square deviation of displacements at specified loads is minimal).

The results of the calculation under loading according to the DCB scheme were compared to the authors' experiment, which was considered in [16]. Samples were made in the same way. The tests were carried out in accordance with GOST R 56815–2015[3] and ASTMD5528–14[4] standards.

The calculation was performed for loading according to the DCB scheme. When calculating dependence $P(\delta)$ for samples without felting, the following stress limits were found and rounded to integer values: Z_t = 39 MPa, X_t = 360 MPa, S = 82 MPa. The obtained values 360 MPa and 39 MPa correspond to the data on the strength of fiberglass specified in [23]. For felting samples (density 10 cm^{-2}), the calculated values were X_t^* = 270 MPa, Z_t^* = 46 MPa and S^* = 97 MPa. Thus, the use of felting made it possible to increase the rupture strength in the Z direction from 39 to 46 MPa (by ~18%).

[3] GOST R 56815–2015. *Polymer Composites. Method for Determination Specific Work of Exfoliation in Tearing Off Conditions.* (In Russ.) URL: https://docs.cntd.ru/document/1200131393/titles (accessed: 22.04.2024).
[4] ASTMD5528M–21. *Standard Test Method for Mode I Interlaminar Fracture Toughness of Unidirectional Fiber-Reinforced Polymer Matrix Composites.* https://doi.org/10.1520/D5528_D5528M-21

When loading according to the DCB scheme, the shear strength limits in the plane XZ S and S^* do not make a big contribution to criterion (4); therefore, values $S = 82$ MPa and $S^* = 97$ MPa obtained in calculations according to the DCB scheme need to be clarified according to the ENF loading scheme. Note that the effect of normal stresses in the X and Z directions is insignificant compared to shear stresses under loading according to the ENF scheme. Therefore, in the calculations, when searching for the values S and S^*, values Z_t, X_t, Z_t^* and X_t^* were taken from solving the inverse problem under loading according to the DCB scheme.

Values $S = 77$ MPa (without felting) and $S^* = 89$ MPa (with felting) were determined from the condition of the best consistency of the experimental and calculated curves $P(\delta)$ (mean square deviation of displacements at given loads is minimal). Evidently, felting made it possible to increase the shear strength in the plane XZ by ~16%.

Figures 12–13 show the experimental "load — displacement" diagrams, as well as calculated dependences $P(\delta)$ for the found values of stress limits:

– $Z_t = 39$ MPa, $X_t = 360$ MPa, $S = 77$ MPa (for control samples without felting);

– $Z_t^* = 46$ MPa, $X_t^* = 270$ MPa, $S^* = 89$ MPa (for samples with felting).

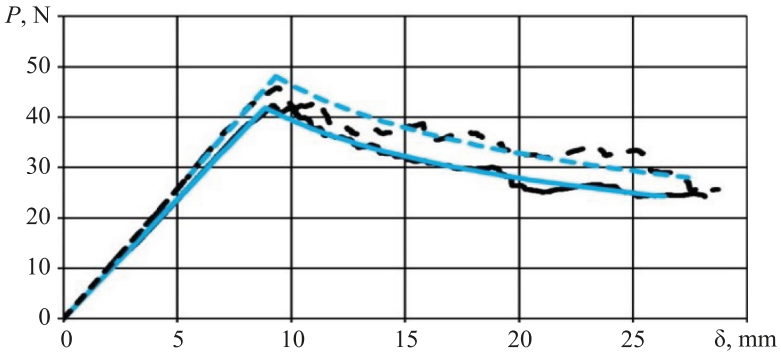

Fig. 12. Experimental diagrams "load – displacement" [16] and calculated dependences $P(\delta)$:
▬ DCB tests of samples without felting; ▬ calculation without felting ($Z_t = 39$ MPa, $X_t = 360$ MPa, $S = 77$ MPa);
- - - DCB tests of samples with felting; - - - calculation with felting ($Z_t^* = 46$ MPa, $X_t^* = 270$ MPa, $S^* = 89$ MPa)

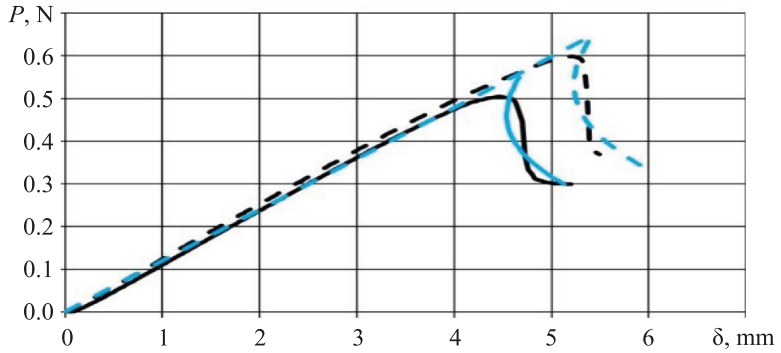

Fig. 13. Experimental diagrams "load – displacement" and calculated dependences $P(\delta)$: ▬ ENF tests of samples without felting;
▬ calculation without felting ($Z_t = 39$ MPa, $X_t = 360$ MPa, $S = 77$ MPa); - - - ENF tests of samples with felting;
- - - calculation with felting ($Z_t^* = 46$ MPa, $X_t^* = 270$ MPa, $S^* = 89$ MPa)

Discussion and Conclusion. Studies of the fabric composite have shown that felting with a density of 10 cm^{-2} increases the viscosity of the interlayer fracture G_{IIc} by ~33%.

Using FEM, the stress state was analyzed in a quasi-static elastic formulation of the problem and with a nonlocal strength theory for the developed numerical models of a beam with cracks of the known length. The distinctive feature of the calculations was that they did not use contact algorithms, but only considered the destruction of the composite layer closest to the crack, and the corresponding change in the area of gluing the layers. That is, the crack was considered as a stress concentrator. The composite strength criterion, which contained three parameters and was recorded through averaged stresses, provided using the method of step-by-step crack advancement to predict the "load — displacement" curve.

The use of felting with a density of 10 cm^{-2} increases the stress limit of the composite in the Z direction by ~18%, and the shear strength in the plane XZ — by ~16%. This became known from solving the inverse problem, i.e., searching for the strength characteristics of the material according to criterion (4) and the "load — displacement" curve.

The results of the presented research will find their practical application. They can be specifically used in problems of forecasting defects, such as delamination (e.g., in low-speed impacts on composites in aircraft skin). The research results will be useful for eliminating these defects with the help of felting.

References

1. Callister WD Jr., Rethwisch DG. *Materials Science and Engineering: An Introduction,* 10th ed. Hoboken, NJ: Wiley; 2018. 992 p. URL: https://www.wiley.com/en-us/Materials+Science+and+Engineering%3A+An+Introduction%2C+10th+Edition-p-9781119405498 (accessed: 22.04.2024).

2. Wei Tan, Falzon BG, Chiu LNS, Price M. Predicting Low Velocity Impact Damage and Compression-After-Impact (CAI) Behaviour of Composite Laminates. *Composites Part A: Applied Science and Manufacturing*. 2015;71:212–226. https://doi.org/10.1016/j.compositesa.2015.01.025

3. Balasubramani Veerappan, S Rajendra Boopathy. Prediction of Residual Tensile Strength of Laminated Composite Plates after Low Velocity Impact. *ARPN Journal of Engineering and Applied Sciences*. 2014;9(3):320–325.

4. Abrate S. *Impact on Composite Structures*. Cambridge: Cambridge University Press; 2009. 289 p. https://doi.org/10.1017/CBO9780511574504

5. Liyong Tong, Mouritz AP, Bannister MK. *3D Fibre Reinforced Polymer Composites.* Amsterdam: Elsevier Science; 2002. 254 p. https://doi.org/10.1016/B978-0-08-043938-9.X5012-1

6. Jinlian Hu. *3-D Fibrous Assemblies: Properties, Applications and Modeling of Three-Dimensional Textile Structures.* Sawston, Cambridge: Woodhead Publishing; 2008. 280 p.

7. Chen Xiaoming, Zhao Yufen, Zhang Chunyan, Wang Xiaoxu, Chen Li. Robot Needle-Punching for Manufacturing Composite Performs. *Robotics and Computer-Integrated Manufacturing*. 2018;50:132–139. https://doi.org/10.1016/j.rcim.2017.09.008

8. Forental GA, Kheruvimov AV, Nikonov AV, Sapozhnikov SB. Stack Fabric Felting to Get PCM G_{IIc} Improvement and LVI Tolerance. *IOP Conference Series: Materials Science and Engineering*. 2021;1024(1):012001. https://doi.org/10.1088/1757-899X/1024/1/012001

9. Sham MS, Venkatesha CS, Jayaraju T. Experimental Methods of Determining Fracture Toughness of Fiber Reinforced Polymer Composites under Various Loading Conditions. *Journal of Minerals and Materials Characterization and Engineering*. 2011;10(13):1263–1275. http://doi.org/10.4236/jmmce.2011.1013099

10. Pinho S, Robinson P, Iannucci L. Developing a Four Point Bend Specimen to Measure the Mode I Intralaminar Fracture Toughness of Unidirectional Laminated Composites. *Composites Science and Technology*. 2009;69(7–8):1303–1309. https://doi.org/10.1016/j.compscitech.2009.03.007

11. Issam Tawk, Jihad Rishmany, Nicolas Saba, Pablo Navarro, Jean-Francois Ferrero. Experimental Study of the Interlaminar Fracture of Composite Materials in Mode III by MSCB Test. *Composite Structures*. 2020;233:111548. https://doi.org/10.1016/j.compstruct.2019.111548

12. Hossein Saidpour, Mehdi Barikani, Multu Sezen. Mode-II Interlaminar Fracture Toughness of Carbon/Epoxy Laminates. *Iranian Polymer Journal.* 2003;12(5):389–400.

13. Sham Prasad MS, Venkatesha CS, Jayaraju T. Experimental Methods of Determining Fracture Toughness of Fiber Reinforced Polymer Composites under Various Loading Conditions. *Journal of Minerals and Materials Characterization and Engineering*. 2011;10(13):1263–1275. http://doi.org/10.4236/jmmce.2011.1013099

14. Ying Zeng, Hong-Yuan Liu, Yiu-Wing Mai, Xu-Sheng Du. Improving Interlaminar Fracture Toughness of Carbon Fibre/Epoxy Laminates by Incorporation of Nano-Particles. *Composites Part B: Engineering*. 2012;43(1):90–94. https://doi.org/10.1016/j.compositesb.2011.04.036

15. Kadhum A, Muslim ZR, Jaffer HI. Interlaminar Fracture of Micro and Nano Composites Special. *Acta Physica Polonica: Series A*. 2019;135(5):1126–1128. http://doi.org/10.12693/APhysPolA.135.1126

16. Forental GA, Sapozhnikov SB. Prospects of Felting Technology for Local 3D-Reinforcement of Polymer Fabric Composites. *Composites and Nanostructures*. 2022;14(56):233–245. https://doi.org/36.10236/1999-7590-2022-14-4-233-245233

17. Maimi P, Gonzalez EV, Gascons N, Ripoll L. Size Effect Law and Critical Distance Theories to Predict the Nominal Strength of Quasibrittle Structures. *Applied Mechanics Reviews*. 2013;65(2):020803. https://doi.org/10.1115/1.4024163

18. Hoang Thai Nguyen, A Abdullah Dönmez, Zdenek P Bazant. Structural Strength Scaling Law for Fracture of Plastic-Hardening Metals and Testing of Fracture Properties. *Extreme Mechanics Letters*. 2021;43(1):101141. https://doi.org/10.1016/j.eml.2020.101141

19. Taylor D. *The Theory of Critical Distances: A New Perspective in Fracture Mechanics.* Amsterdam: Elsevier Science; 2007. 306 p. https://doi.org/10.1016/B978-0-08-044478-9.X5000-5

20. Mahmoodi MJ, Khamehchi M. Finite Element Analysis of Free Corner Effects in Composite Laminates Based on a Global–Local Model. *Archive of Applied Mechanics*. 2023;93(12):4327–4350. http://doi.org/10.1007/s00419-023-02494-1

21. Jaehong Lee, Zafer Gurdal, O Hayden Griffin Jr. Layer-Wise Approach for the Bifurcation Problem in Laminated Composites with Delaminations. *AIAA Journal*. 1993;31(2):331–338. https://doi.org/10.2514/3.11672

22. Sapozhnikov SB. Failure of Fabric Reinforced Composite with Concentrators: Implementation of Inelastic Deformation in Numerical Simulation. *Composites and Nanostructures*. 2020;12(45):31–39. https://doi.org/10.36236/1999-7590-2020-12-2-31-39

23. Barbero EJ. *Introduction to Composite Materials Design*, 2nd ed. Boca Raton: CRC Press; 2011. 562 p. https://doi.org/10.1201/9781439894132

About the Authors:

Galina A. Forental, Research Engineer, South Ural State University (76, Lenin Ave., Chelyabinsk, 454080, Russian Federation), SPIN-code, ORCID, ScopusID, gforental@mail.ru

Sergey B. Sapozhnikov, Dr.Sci. (Eng.), Professor of the Engineering Mechanics Department, South Ural State University (76, Lenin Ave., Chelyabinsk, 454080, Russian Federation), Leading Scientist, Central Aerohydrodynamic Institute named after N.E. Zhukovsky (1, Zhukovsky Str., Zhukovsky, Moscow Region, 140180, Russian Federation), SPIN-code, ORCID, ScopusID, ResearcherID, sapozhnikovsb@susu.ru

Claimed Contributorship:

GA Forental: conducting experiments and calculations, analysis of the research results, formulation of conclusions, text preparation, layout of the paper.

SB Sapozhnikov: academic advising, revision of the text.

Conflict of Interest Statement: **the authors declare no conflict of interest.**

All authors have read and approved the final manuscript.

Об авторах:

Галина Анатольевна Форенталь, инженер-исследователь Южно-Уральского государственного университета (454080, Российская Федерация, г. Челябинск, пр. Ленина, 76), SPIN-код, ORCID, ScopusID, gforental@mail.ru

Сергей Борисович Сапожников, доктор технических наук, профессор Южно-Уральского государственного университета (454080, Российская Федерация, г. Челябинск, пр. Ленина, 76), ведущий ученый Центрального аэрогидродинамического института имени профессора Н.Е. Жуковского (140180, Российская Федерация, г. Жуковский, Московская область, ул. Жуковского, 1), SPIN-код, ORCID, ScopusID, ResearcherID, sapozhnikovsb@susu.ru

Заявленный вклад авторов:

Г.А. Форенталь: проведение экспериментов и расчетов, анализ результатов исследований, формулирование выводов, подготовка текста статьи, оформление статьи.

С.Б. Сапожников: научное руководство, корректировка текста статьи.

Конфликт интересов: **авторы заявляют об отсутствии конфликта интересов.**

Все авторы прочитали и одобрили окончательный вариант рукописи.

Received / Поступила в редакцию 03.06.2024
Reviewed / Поступила после рецензирования 27.06.2024
Accepted / Принята к публикации 05.07.2024